# THIN PLY COMPOSITES: EXPERIMENTAL CHARACTERIZATION AND MODELING

R. Amacher , J. Cugnoni *, J. Botsis
Lab. of Applied Mechanics and Reliability Analysis, EPFL, Lausanne, Switzerland
* Corresponding author (joel.cugnoni@epfl.ch)

**Keywords**: *thin-ply composites, size effects, finite element, testing, failure mechanisms*

## Abstract

Thin ply composites are quickly gaining interests in the composite industry not only because of the larger design space that they offer but also because of positive size effects that have been shown to affect their performance in various loading conditions [1]. In this work, carbon-epoxy composites of different ply thicknesses (30g/m$^2$, 100g/m$^2$ and 300g/m$^2$ fiber areal weight) were produced from the same batch of Toray M40JB fiber and NorthTPT TP80ep matrix to study the influence of ply thickness on the ultimate strength and onset of damage of lamina and quasi isotropic laminates. Characterization tests on unidirectional lamina showed only limited influence of the ply thickness on the elastic and ultimate strength properties except for longitudinal compression in which the thinner ply specimens showed some advantage because of a more uniform microstructure. Uniaxial tension, open-hole compression and open-hole tensile fatigue tests on quasi isotropic $[45°/90°/-45°/0°]_{ns}$ laminates showed however very significant improvements of on-set of damage, and in some cases ultimate strength, when decreasing the ply thickness. These performance improvements could be related to a major change in the damage progression and failure modes of the laminates caused by a systematic delay or near suppression of transverse cracking and delamination growth in thin-ply composites. Detailed meso-scale finite element models of quasi isotropic unnotched tensile tests were developed and demonstrated that the increased stability of transverse intralaminar cracks was the main cause of the improved onset of damage of thin ply composites.

## 1 Introduction

In the recent years, important progresses have been made in developing composite laminates using thinner plies. Nowadays, thin ply composite materials are commercially available down to about 20 micrometer per ply depending on the type of fiber. The motivation for this trend towards thinner plies is not only to allow producing thinner and lighter laminates and structures but also to provide enhanced strength and damage resistance thanks to positive size effects and increased design space.

The first benefit of using thinner plies in a given structure, i.e at a constant laminate thickness, is the ability to use a larger number of ply orientations to achieve a better solution as the laminate design space is naturally extended. This fact is particularly important for already thin laminates in which only two or three fiber orientations can be selected to satisfy classical design constraints such as laminate symmetry, minimum fraction of fibers at 90° and available prepreg thickness. For example, using 30g/m$^2$ thin-ply prepregs instead of a 300g/m$^2$ standard prepregs in a 0.9 mm composite skin allows the designer to propose optimized laminates such as $[0°/45°/90°/-45°/0°]_{3s}$ (or more complex) instead of a basic [0°/90°/0°] cross-ply for example.

The second benefit is that thin-ply composite may present some advantages due to positive size effects with respect to decreasing ply thickness. The first comprehensive research work on mechanical performance of thin-ply composite materials has been carried out by Tsai et al. [1]. In their research, thin-ply (0.04 mm ply) and thick-ply carbon-epoxy composites (0.2 mm ply) have been subjected to quasi-isotropic unnotched tensile tests in static and fatigue loading, quasi-isotropic open-hole tensile tests in static and fatigue loading and finally to post-impact damage compression test. Unnotched tensile tests of quasi isotropic laminates have shown that the thin-ply laminates exhibits a significantly higher ultimate strength (+10%) than the thicker ply ones. The thick-ply specimens showed a significant

damage before ultimate failure while the thin-ply ones remained linear elastic until the fracture load. Thanks to the reduction of the damage developed close to the free-edge of the specimen, a better fatigue behavior and post-fatigue resistance of thin-ply composite was also observed. After 50'000 fatigue cycles, the thin-ply composite did not show any significant strength reduction while the thick ply composite already failed at a 30% lower stress.

Open-hole tensile tests of quasi-isotropic specimens have shown the same trend: the thin-ply laminate really limits the development of damage around the hole and prevents the propagation of large delamination cracks. On the contrary, the "thick" laminate failed by progressive delamination and transverse microcracking of the matrix and lost linearity at a relatively lower stress. However the ultimate stress of the thicker laminate in open-hole test appears slightly higher than the thin one. Reduced damage progression around the hole was also observed by X-Ray imaging during fatigue open-hole tensile tests.

Moreover, a significantly reduced delamination area was observed after impacting a thin-ply quasi-isotropic laminate. This delamination damage reduction helped the thin-ply specimens to maintain a better stability than "thick" ones in post-damage compression tests. Overall, because of reduced free-edge effects and thus delayed delamination, thin-ply composite exhibited generally a much more durable performance and appeared less sensitive to initial damage than thicker ply laminates.

To explain the observed changes in the mechanical performance of thin-ply composites, several sources of size effects could be considered [2-4]:

1. Volume & probability of critical defects: similarly to size effects in fibres, the strength of a composite part may be related to the probability of finding a critical defect (weakest link assumption). As the volume of material was kept constant in the experiment of Tsai et al., this volumetric size effect is not expected to play a role and does not explain the presence of positive size effects.
2. Crack propagation controlled mechanisms: according to Linear Elastic Fracture Mechanics (LEFM), the ultimate strength of a composite structure in which the dominant mode of failure is crack propagation is expected to be inversely proportional to the square root of the characteristic size of the crack, which, in the case of an intra laminar crack constrained by the surrounding plies, is equal to the ply thickness [3-4]. To represent this effect, the concept of in-situ strength of a ply has been proposed by Camanho et al. [5] based on the stability of transverse cracks of a ply constrained by neighboring plies of different orientations.
3. Laminate scaling: the scaling up in laminate thickness can be achieved by either changing the number of identical plies in the laminate thickness (laminate block scaling, for example $[0°_n/45°_n/-45°_n/90°_n]_s$) or by repeating the lay-up sequence several times using a single ply for each orientation (sub-laminate scaling, for example $[0°/45°/-45°/90°]_{ns}$). These two types of laminate thickness scaling strategies have been shown [3] to give very different results because of triggering of different failure mechanisms. Using sub-laminate scaling was shown to provide a higher strength in some specific load cases such as unnotched tension as it tends to reduce the stress concentration at the free edges and thus delays the delamination of the plies. However, an early and more brittle failure mechanism has been reported in open-hole tension [6-8] when using sub-laminate scaling when compared to ply-block scaling.
4. Microstructure and processing: the manufacturing of a composite part is not a fully scale independent process. Residual strains, fibre alignment and waviness, porosity and the amount of fibre clustering and resin rich zones tend to increase in larger and thicker structures, thus introducing another kind of size effect which is closely related to the production process [2,9,10].

| Test | Stacking | *Thin* | *Intermediate* | *Thick* | L [mm] | b [mm] | t [mm] |
|---|---|---|---|---|---|---|---|
| Unnotched tensile UD 0° | UD $[0°_n]$ | *n=40* | *n=12* | *n=4* | 250 | 15 | 1.2 |
| 0° compression (Sandwich beam) | $[0°_n]$/core/$[0°_n]$ | *n=20* | *n=6* | *n=2* | 440 | 20 | 1.2 |
| ILSS | UD $[0°_n]$ | *n=130* | *n=39* | *n=13* | 23.4 | 7.8 | 3.9 |
| Unnotched tensile | QI, $[+45°/90°/-45°/0°]_{ns}$ | *n=10* | *n=3* | *n=1* | 240 | 24 | 2.4 |
| Quasi isoptropic | QI, $[+45°_{10}/90°_{10}/-45°_{10}/0°_{10}]_{ns}$ | | | *n=1* | 240 | 24 | 2.4 |
| | QI, [+45°/+67.5°/90°/-67.5°/-45°/-22.5°/0°/+22.5°]ns | | | *n=5* | 240 | 24 | 2.4 |
| OHT Quasi isotropic | QI, $[+45°/90°/-45°/0°]_{ns}$, n=10, THIN | *n=10* | | *n=1* | 240 | 36 | 2.4 |
| OHC Quasi isotropic | QI, $[+45°/90°/-45°/0°]_{ns}$, n=20, THIN | *n=20* | *n=6* | *n=2* | 125 | 25 | 4.8 |

*Table 1: Specimen dimensions and stacking sequences*

According to the available literature on size effects, thin-ply composite are expected to offer better performance than standard composite materials. However, only limited literature is available today on the performance of thin-ply composite materials and validated models to predict the thin-ply size effects are still lacking. Moreover, the pioneering articles on the performance of thin-ply composites mostly dealt with unidirectional thin-ply prepreg based laminates [1, 11-13] but more recent works have shown similar benefits for non-crimp fabrics [14].

The objective of the present work is to quantify experimentally the performance of a commercially available thin-ply composite material at the ply level, laminate level and component level and highlight the effects of ply thickness on the measured mechanical properties. A specific attention is paid to the characterization of the damage onset and to the study of the sequence of damage mechanisms. A detailed meso scale finite element modeling approach is proposed to explain and predict the effects of ply thickness on the onset of damage and strength of quasi-isotropic laminates in uniaxial tension.

## 2 Materials and Methods

In the present study, unidirectional prepreg tapes with three different fiber areal weight (300[1], 100 and 30 g/m2) were produced at North-TPT Switzerland using M40JB fibers and ThinPreg$^{TM}$ 80EP/CF epoxy resin, using the same fiber and resin production batches on the same production line in order to minimize potential scatter.

Following ASTM standards, unidirectional, quasi-isotropic $[45°/90°/-45°/0°]_{ns}$ specimens were produced in autoclave using the recommended curing cycle (80°C, 8h, 5atm peak pressure). To achieve a reproducible fiber volume fraction of 55% and uniformity of the specimen thickness, a mold consisting of two rigid and perfectly planar aluminium plates separated by precisely machined spacers were used for the production. The consolidated ply thicknesses for 55%vol fiber were determined in a preliminary study using optical microscopy and image processing techniques for the evaluation of the fiber volume fraction. Throughout the study, the fiber volume fraction of each plate produced was calculated from its total fiber weight and thickness and the test results were then normalized to 55% volume fraction.

As the main objective of this work was to study ply thickness effect, the chosen scaling method was to keep all specimen dimensions constant and only change the ply thickness in order to avoid volumetric size effects. Sub-laminate scaling (repetition of a lamination sequence) was considered for all test cases and other approaches like half-angle quasi-isotropic laminates, ply block scaling and

| Property | Unit | Thin 30g/m$^2$ value | Intermediate 100g/m$^2$ value | Thick 300g/m$^2$ value |
|---|---|---|---|---|
| Tensile modulus @ 0° | [GPa] | 222 | 223 | 229 |
| Ultimate tensile strength @ 0° | [MPa] | 2250 | 2350 | 2360 |
| Tensile onset of damage @ 0° | [MPa] | 1644 | 2019 | 1391 |
| Poisson's ratio $\nu_{12}$ | - | 0.314 | 0.274 | 0.266 |
| Tensile modulus @90° | [GPa] | 7.01 | | |
| Ultimate tensile strength @90° | [MPa] | 23 | | |
| Compressive modulus @ 0° | [GPa] | 213 | 201 | 208 |
| Chord tensile modulus @ 0° | [GPa] | 231 | 203 | 225 |
| Ultimate compressive strength @ 0° | [MPa] | 1052 | 869 | 848 |
| Compressive modulus @90° | [GPa] | 80.4 | | |
| Ultimate compressive strength @90° | [MPa] | 117 | | |
| Interlaminar shear strength | [MPa] | 79.1 | 79.91 | 76.73 |
| In-plane shear modulus | [GPa] | 4.661 | | |
| Maximum in-plane shear stress | [MPa] | 88.263 | | |
| In-plane shear stress at 0.2% offset | [MPa] | 50.231 | | |
| Mode I interlaminar fracture toughness at initiation | [J/m$^2$] | 139 | | |
| Mode II interlaminar fracture toughness at initiation | [J/m$^2$] | 445 | | |

*Table 2: Lamina level properties*

[1] *Two 150 g/m$^2$ tapes stacked together*

optimized orthotropic laminate sequences were tested for comparison in a few conditions. Additional unnotched tension tests on quasi-isotropic laminates with different number of sub-laminate repetitions ($[45°/90°/-45°/0°]_{ns}$ with $n$=10 and $n$=3 for 30 g/m2), and thus different thicknesses, were also performed to differentiate the effects of sub-laminate scaling and ply thickness effects.

Following MIL17 approach, the test matrix consisted firstly in a series of ply level characterization tests, namely longitudinal and transverse tensile and compression tests (ASTM D3039 and D5467) as well as in-plane and interlaminar shear tests (ASTM D3518 and D2344-84). Secondly, laminate level and component level properties were measured through unnotched tensile tests (ASTM D3039), open-hole compression test (ISO 14126/ASTM D6484) and open-hole tensile fatigue tests (ASTM D5766 and D7615) on quasi-isotropic laminates. In all cases, the test batch size was chosen to be between to 5 and 10 specimens.

In most tests, the specimens were equipped with resistive strain gages and the measurements were complemented with acoustic emission monitoring to determine the onset of damage based on the measured cumulative acoustic energy signal. A 65db acquisition threshold was set on Mistras-2001 acoustic emission monitoring system to filter parasitic acoustic noise during the experiment and only the acoustic events detected within the specimen gage length were kept for analysis. Selected specimens were also investigated using digital image correlation and ultrasonic c-scan. The microstructure and void fraction of representative batches were also inspected by optical micrography analysis and showed negligible porosity in all cases.

Finally mode I & II interlaminar delamination tests were also carried out using standard double cantilevered beam (DCB, ASTM D5528-01) and 4 point end-notched flexure tests to provide consistent data for damage modeling.All specimen dimensions for tests on laminates are presented in Table 1.

## 3. Experimental results

*Ply level properties*

The measured unidirectional ply level properties are summarized in Table 2. It should be noted that in those tests the same specimen thickness was used for the different ply thicknesses and thus these results do not represent test results on a single isolated ply. Overall no significant differences were found between the different lamina level properties of thin (30g/m$^2$), intermediate (100g/m$^2$) and thick plies (300g/m$^2$) composites. All measured elastic and strength properties were found to be in the expected range for M40JB fibers at 55% volume fraction and are perfectly comparable with other similar composite materials.

However, one notable exception was found for the compressive strength of unidirectional laminates, in which a clear trend was observed (Fig. 1). In this test, the thin-ply, intermediate and thick materials exhibited an average ultimate compressive strength of 1052 MPa, 869 MPa and 848 MPa respectively. Despite the large scatter seen in this test, the trend towards an increased compressive strength when decreasing ply thickness appears clearly.

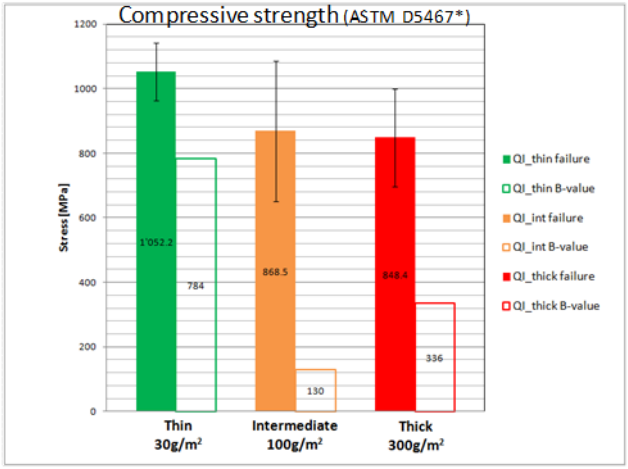


*Fig. 1: unidirectional compression strength vs ply thickness showing a positive increasing trend for thinner ply laminates*

To understand the cause of this change, optical micrographs of thin-, intermediate- and thick-ply unidirectionnal specimens were analyzed and are presented in Fig. 2. The microstructure of the thick laminate was found to be fairly inhomogeneous with regions of higher and lower fiber volume fractions (in the range of 42% to 64 %vol fiber) which could be attributed to fiber rearrangement and resin flow during the low-viscosity phase of the curing cycle. However, as show in Fig. 2, when the ply size was decreased to 100g/m$^2$, a better uniformity of the microstructure was achieved but the individual layers could still be identified. Finally for the thinnest plies, the microstructure was found to be even more homogeneous up to the point that it

became difficult to identify the interfaces between the plies as the ply thickness corresponded to just a few fiber diameters. These significant differences in microstructure may explain the relatively poor results of the thick ply specimen with respect to the thinnest ones as the resin rich regions are inherently more prone to fiber micro buckling and thus could be sites for early development of compressive instability of the UD laminate.

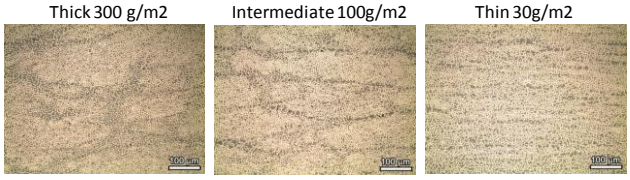


*Fig. 2: microstructure of unidirectional laminates for different ply thickness showing a significant difference in the degree of heterogeneity of local fiber volume fractions, i.e visible fiber bundles and resin rich regions in thick ply vs uniform microstructure for thin ply.*

*Unnotched laminate properties*

On the laminate level, the tensile tests performed on quasi-isotropic plates showed a great sensitivity to ply thickness and/or number of sub-laminate repetitions *n* as shown in Table 3 and graphically in Fig. 3. Indeed, a clear increase of the unnotched tensile strength was observed from 595 MPa for thick-ply (*n*=1), to 832 MPa (+39%) and 847 (+42%) respectively for intermediate (*n*=3) and thin-ply (*n*=10) materials. As shown in Fig. 4, the thick-ply specimens failed in a very progressive manner starting by transverse and shear cracking of the 90° and +/-45° plies accompanied by massive delamination and finally 0° ply failure. The intermediate-ply specimen showed also a multiple mode of failure but with a more limited delamination area and a more abrupt final failure by propagation of macroscopic cracks perpendicular to the load direction. The thin-ply specimens all failed in a quasi-brittle manner exhibiting no sign of damage before final failure by propagation of a single macroscopic crack perpendicular to the load direction. This complete change of the damage mechanism development sequence with ply size / sub-laminate repetitions clearly explains the measured strength increase when decreasing the ply thickness.

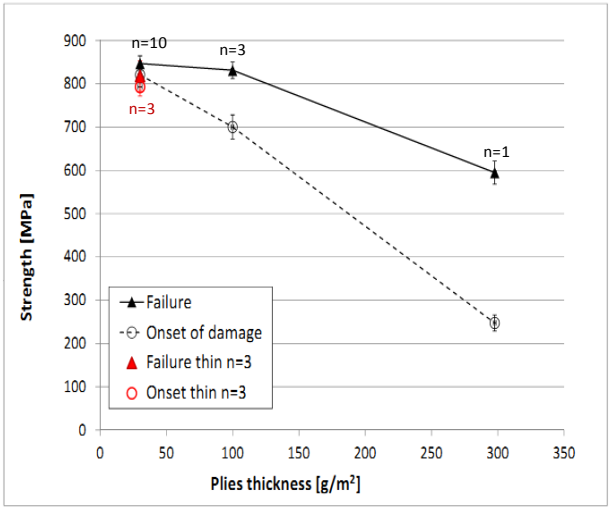


*Fig. 3: Ultimate strength and onset of damage with respect to ply thickness in unnotched quasi-isotropic tensile tests*

The stress at onset of damage was also identified by acoustic emission monitoring and was defined as the stress at which the cumulative acoustic energy signal starts becoming significant (threshold $10^{-15}$ nJ), which corresponds to the occurrence of the very first damage mechanisms (i.e no change of stiffness at this point). The measured damage initiation point was found to be only 248 MPa for thick-ply laminates while intermediate- and thin-ply reached respectively 702 MPa and 822 MPa when using sub laminate scaling. So, in addition to a strong ultimate strength increase, the thin-ply laminates exhibited an even larger increase of stress at damage initiation (+220%) when compared to thick-ply laminates. It is also remarkable that with the thinnest plies, the measured onset of damage was found just 3% below the ultimate strength meaning that nearly no damage occurred before final failure and thus that a laminate with 30g/m$^2$ ply thickness is close to the asymptotic behavior.

| Test | Property | Unit | Thin (30g/m$^2$) sublaminar stacking $[45°/90°/-45°/0°]_{10s}$ | Thin (30g/m$^2$) ply level stacking $[45°_{10}/90°_{10}/-45°_{10}/0°_{10}]_s$ | Intermediate (100g/m$^2$) sublaminar stacking $[45°/90°/-45°/0°]_{3s}$ | Thick (300g/m$^2$) $[45°/90°/-45°/0°]_{1s}$ |
|---|---|---|---|---|---|---|
| UNT | Ultimate tensile strength | [MPa] | 847 | 532 | 832 | 595 |
| | Tensile onset of damage | [MPa] | 821 | 305 | 701 | 248 |
| OHT | Far field ultimate strength | [MPa] | 380 | | | 545 |
| | Far field stress at the onset of damage | [MPa] | 352 | | | 255 |
| | # cycles to ruin (-10% app. stiffness) at 316 MPa | | > 1e6 | | | < 2e4 |
| OHC | Ultimate open-hole compressive strength | [MPa] | 255.3 | 189.1 | 229.7 | 215.9 |
| | Open hole onset of damage | [MPa] | 226 | 155 | 200 | 192 |

*Table 3: Specimen dimensions and stacking sequences*

Interestingly, the intermediate ply thickness laminate showed already a comparable strength compared to the thin-ply one but is not yet as good in terms of damage onset. Thus it seems from these results that the minimum ply thickness required to reach an optimal damage onset is smaller than that required to reach the optimal strength.

Moreover, it should be noted that only little difference in onset of damage and ultimate strength was observed between ply block scaling laminates based on thin-ply prepregs and thick ply laminates, which demonstrates that the effect observed was not related to changes in intrinsic ply properties.

Overall, it appears from those results that when using the thinnest plies with sub-laminate scaling, the damage response of the composite becomes similar to that of a homogeneous and brittle solid which does no more exhibit the early first ply failures and delamination propagation seen traditionally in composites.

To distinguish the effects of ply thickness and sub laminate scaling, additional unnotched tensile tests were performed on thin-ply 30g/m$^2$ quasi-isotropic specimens with $n$=3 sublaminate repetitions instead of $n$=10 (red symbols on Fig. 3). No significant differences were found between $n$=3 and n=10 laminates for the thinnest ply specimens (30 g/m2) and both series of specimens showed a nearly coincident onset of damage and ultimate failure strength. However, comparing the $n$=3 laminates for 100g/m2 and 30g/m2 plies, a clear trend could be observed. Indeed, the thinnest ply laminates exhibited a 12% higher stress at onset of damage (790MPa vs 700 MPa) than the intermediate ply thickness but a statistically equivalent ultimate strength. Overall, these results suggest that the onset of damage is mostly related to the ply thickness as it is proposed in the in-situ strength model of Camanho [5] for example. On the contrary, according to the present results, it remains still unclear whether the ultimate tensile strength of the laminate depends more on the number of sub laminate repetitions $n$ or on the ply thickness.

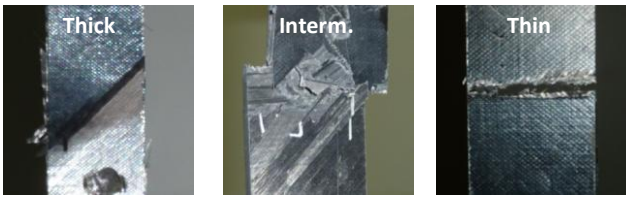


*Fig. 4: Failure modes observed in quasi-isotropic uniaxial tensile tests: transverse cracking and delamination failure for thick (n=1), multimode failure for intermediate (n=3) and fiber dominated failure for thin ply laminates (n=10)*

### *Notched laminate properties*

Notched "open hole" tests were performed on quasi-isotropic specimens in quasi-static tension and compression as well as tensile fatigue. The quasi-static notched compression tests have shown a strength improvement by 18% for the thin-ply laminates ($n$=20, 255 MPa) versus the thick ply ones ($n$=2, 216 MPa). This small increase is comparable to what was reported previously in [7,8] for sub-laminate scaling. Moreover, it should be noted that the observed failure modes for the thick ply was a combination of intra laminar cracking in the 45° plies , fiber kinking and delamination while in thin

ply specimens failure occurred within a localized band of lateral fiber kinking.

On the other hand, in quasi static open hole tensile tests the thin-ply specimens (30g/m$^2$, $n$=10) reached a 34% lower ultimate strength (380 MPa) than the thick-ply laminates (300g/m$^2$, $n$=1, 545MPa). Comparison of the failure modes clearly showed a transition from multi-mode failure in thick-ply laminate towards a brittle macroscopic transverse crack initiated at the apex of the hole in the thin-ply composite. This failure mode transition corresponds well to the observations and explanation given in [6]. Indeed, these results could be explained by the absence of early damage growth in the thin-ply composite which did not allow for local stress relaxation around the apex of the hole and thus leads to a premature brittle failure when compared to the thicker-ply composite. This is thus a particular case where damage progression actually improves the ultimate strength of the component. The onset of damage measured in open-hole tensile tests were 352 MPa and 255 MPa for thin-ply respectively thick-ply laminates, thus demonstrating an opposite tendency to what was observed for ultimate strength (+31% increase for thin-ply). Indeed, comparing the measured onset of damage (352 MPa) to ultimate strength (380 MPa), it appears clearly that thin-ply composites failed without significant damage progression in open-hole tension. On the other hand, in thick specimens, damage started very early on, at approximately 50% of the ultimate strength.

Fatigue tests were also carried out on open-hole tension specimens and were performed in load control for up to 1 million cycles. The fatigue loading ratio was chosen purely tensile and set to $R$=0.1. During the test, load and displacement peaks were recorded for each cycle and the stiffness of the samples were monitored over time. The end of life was considered reached when the specimen stiffness attained 90% of its initial value. Peak stress values of 277 MPa, 316 MPa and 342 MPa were considered for the thin-ply specimens which corresponded to 90%, 83% and 73% of their ultimate strength in static open-hole tension tests. Thick-ply laminates were tested in fatigue at 277MPa, 316 MPa and 361 MPa peak stress, which corresponded respectively to 50% , 58% and 66% of ultimate strength. In these tests (Fig. 5), thick-ply composites (300g/m$^2$, $n$=1) exhibited a progressive damage accumulation by delamination and transverse / shear cracking of 90° and +/-45° plies leading to ruin after about 10k cycles at 361MPa, before 20k cycles at 316 MPa and 108k cycles at 277 MPa. As expected, on a typical fatigue S-N plot (Fig. 5), a clear fatigue life reduction trend can be seen for thick-ply composites. Thin-ply composites (30g/m$^2$, $n$=10) on the other hand showed a very particular behavior: even though thin ply laminates failed after about 8k cycles at 342 MPa (90% of ultimate strength), almost no stiffness degradation could be observed at peak stresses lower or equal to 316 MPa (i.e 83% of ultimate strength) after up to 1 million cycles. On an S-N diagram (Fig.

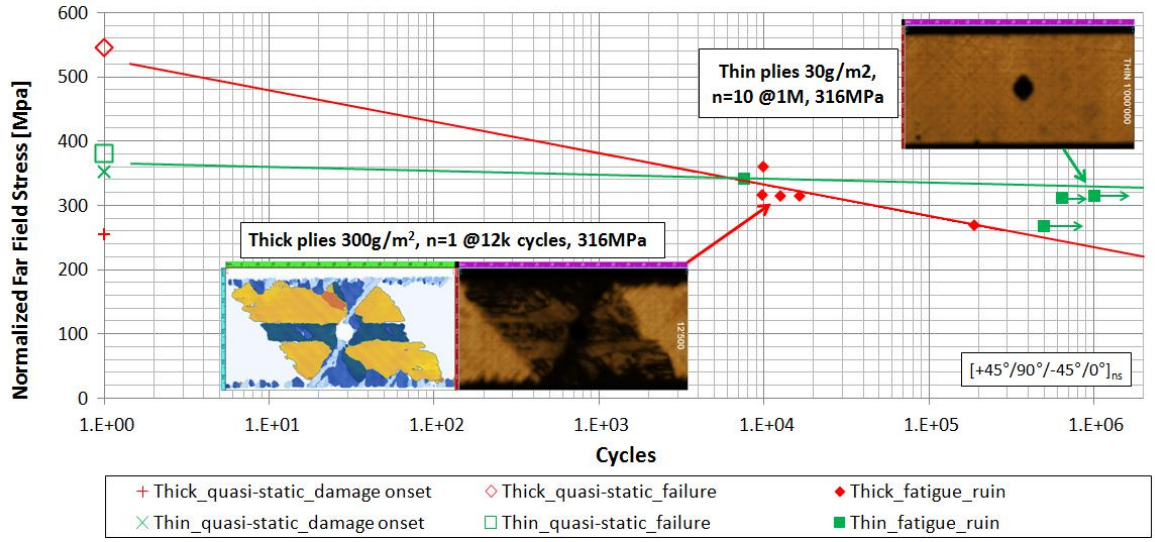


*Fig. 5: Open hole tensile fatigue test results and corresponding ultrasonic c-scan damage inspection images*

5), the fatigue behavior of thin-ply laminates exhibits a clear fatigue limit, at about 320 MPa, below which little to no damage develops and thus nearly "infinite" life can be reached. Interestingly, the onset of damage in quasi static open hole tension was measured at 352 MPa, which was very close to the apparent "infinite" fatigue limit for thin-ply laminate. Contrarily, the faster fatigue damage growth in thick-ply specimens could be explained by the fact that the chosen stress levels were significantly higher than their onset of damage. Comparing the fatigue lives measured at 316 MPa for thick-ply (<20k cycles) and thin-ply laminates (>1M cycles), it appears clearly that thin-ply laminates (also with high *n*) provide a significant advantage in terms of durability.

According to the present results, for a composite structure in which durability or first damage is driving the design, it appears clearly that thin-ply composites with high sub-laminate repetitions provide clear performance improvements, even in the presence of open holes under tension loading.

## 4. Finite element analysis

To understand the mechanisms leading to the observed changes in damage progression when decreasing ply thickness, detailed meso-scale three-dimensional finite element models were developed. As the main cause of thin-ply size effect appear to be related to the coupled stability of intra-laminar transverse cracks and inter-laminar delamination cracks at the free edges of the composite [1,3,5,6], the models had to represent multiple competing damage mechanisms in order to capture the complex damage progression seen in quasi-isotropic laminates. In this series of model, it was assumed that all constitutive properties of the UD lamina and all interfaces were size independent and thus potential size effects could only be related to the geometry of the ply thickness and geometry of the laminate. A 3D continuum finite element model of the unnotched quasi-isotropic tensile tests of both thick-ply (300g/m2, $[45°/90°/-45°/0°]_{1s}$) and intermediate ply thickness specimens (100g/m2, $[45°/90°/-45°/0°]_{3s}$) were developed using Simulia Abaqus Explicit v6.10 in which each ply was discretized using 3D 8 node hexahedral elements with reduced integration (C3D8R). The ply behavior was modeled using a transverse isotropic elastic model with Hashin failure criterion in which only the fiber failure part was active to capture the 0° ply failure (implement as a VUMAT). In each ply, cohesive elements were inserted at predefined locations to represent localized intra-laminar transverse cracks propagating parallel to the fibers (shear or transverse cracking). The cohesive behavior was modeled by assuming a linear stiffness degradation and critical energy release rates (ERR) in mode I and II equal to those measured in inter-laminar delamination tests (DCB and 4ENF) as well as a power law of exponent 2 for mixed mode ERR. The critical tensile and shear stress of the cohesive law were considered equal to the transverse tensile strength and in-plane shear strength of the UD plies. The uncoupled normal and shear stiffness coefficients of the cohesive elements were calculated such as to be equivalent to the continuum transverse normal and shear stiffness. Finally, inter-laminar cohesive interfaces were modeled in a similar manner using the experimentally determined fracture energies in mode I and II. All constitutive properties used in the modeling were based on the measured values found in Table 2.

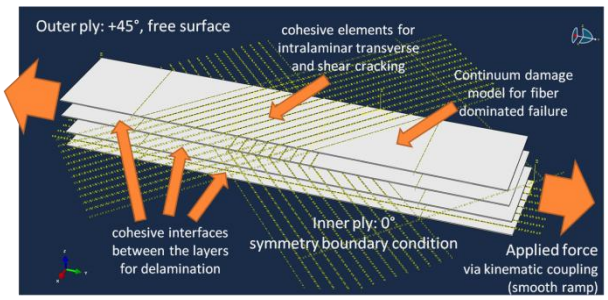


*Fig. 6: 3D finite element modeling strategy*

In order to capture the quasi-static behavior of the specimens using an explicit dynamic simulation, an automatic mass scaling strategy was used. The target stable time increment was determined via a convergence study based on the overall energy balance in order to ensure that kinetic energy remained less than 0.2% of strain energy and significantly lower than total damage energy until ultimate failure. According to the symmetry of the problem, the whole specimen length and width were modeled (240x24mm) while only one half of the specimen thickness (1.2mm) was considered, the other half being replaced by symmetry boundary conditions. The loading conditions were modeled as two opposite concentrated forces on reference points

coupled to the end surfaces of the specimen. A smooth step loading function was used to minimize inertia effects.

As proposed in the in-situ strength model of Camanho [5], the shift in transverse normal and shear cracking of thin-ply laminates may be related to the stability of transverse intra-laminar crack and thus to the crack opening displacement within such cracks. To model this potential mechanism, a mesh with a substantial refinement within the thickness of each ply is required in order to capture the actual curvature of the crack surface. A mesh convergence study was thus carried out to determine both the appropriate in-plane and through the thickness characteristic mesh size. As a result, it was shown that at least 6 to 8 linear hexahedral elements are required in the thickness of each ply in order to capture the aforementioned effect. However, the model was shown to be much less sensitive to the in-plane mesh size and a 0.5 mm in-plane element characteristic size was sufficient to reach a convergence. Different arbitrary patterns of predefined intra-laminar cracks (cohesive element lines) were also tested to ensure that the results were independent of this parameter.

The final FE models for the thick and intermediate ply quasi isotropic unnotched tension tests ($[45°/90°/-45°/0°]_{ns}$ with $n$=1 and $n$=3 resp.) corresponded to meshes with 112'842 nodes / 92'820 elements and 771'731 nodes / 639'864 elements respectively. Simulation times were in the order of 3h on 6 processors for the thick-ply specimen and about 24h on 16 processors for the intermediate-ply model.

Based on the simulation results, several indicators were identified using definitions as close as possible to those used in the real tests. The on-set of damage was determined from the stress vs damage energy graph using a damage energy threshold. The ultimate strength was determined from the stress-strain curve by the intersection between the elastic tangent at origin and the tangent line at failure (Fig. 6).

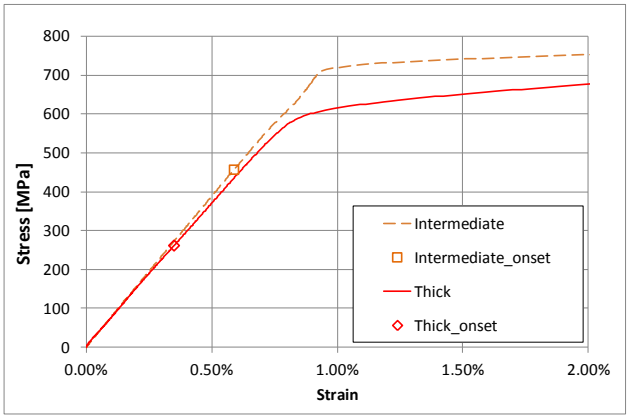


*Fig. 6: Simulated stress-strain curve for the thick (300 g/m$^2$, n=1) and intermediate- ply thickness (100 g/m$^2$, n=3) quasi isotropic unnotched tensile test.*

*Results & Discussion*

First of all the chronology of the different damage mechanisms has been studied in details for the case of the thick ply laminate and compared to two c-scan performed on interrupted tests (Fig. 7). After about 50% of the ultimate load (~ 253 MPa), the first damage starts by intra-laminar transverse cracking with an initiation triggered by normal stresses (mostly mode I) in the 90° ply. Then, intra laminar shear damage develops progressively from both sides of the specimen and is followed closely by the development of limited interlaminar cracks at the free edges propagating mostly in mode II. Delamination cracks appeared to be triggered by local shear stress concentrations in the surrounding of the intra laminar transverse cracks near the free edges and propagated preferentially at the interface between the +/-45° and 90° plies. Damage progression then accelerated at about 500MPa when extensive transverse cracks in the +/-45° plies had developed. Several fronts of inter laminar cracks propagated towards the center of the specimen. Finally, at about 600MPa and after massive delamination and transverse cracking, the +/-45° and 90° plies completely lost their loading capabilities and thus only the 0° ply remained to carry the applied load. As a result, the 0° ply became quickly overloaded and finally broke by fiber failure at 609 MPa. The extensive delamination and intra laminar cracking predicted by the model corresponded well to the type of failure observed experimentally (Fig. 4).

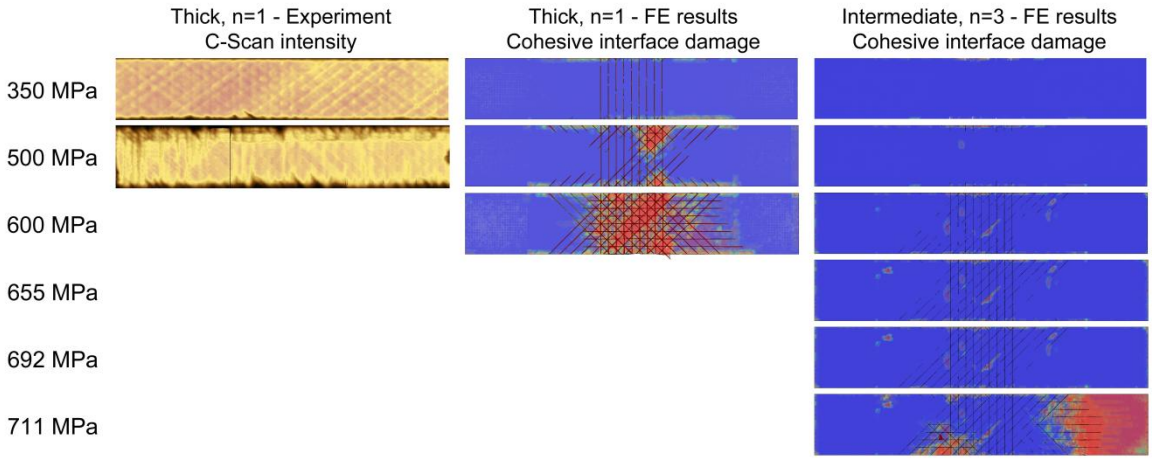


*Fig. 7: measured and simulated cohesive element damage progression showing clearly the propagation of transverse cracks and delamination initiated at the free edges of the specimen.*

In the case of the intermediate laminate, a different damage evolution scenario was observed. First of all, minute local damages (on about 50 elements) were observed in the early stage of loading. These early damages were particularly observed in regions where cohesive element lines of two neighboring plies overlapped and were thus considered as modeling artifacts caused by stiffness mismatch between the cohesive and continuum elements. However, after these early damage initiations, no significant damage propagation was observed until ~500 MPa where intralaminar transverse cracking started to grow very slowly in the 90° ply from the free edges. Very limited propagation of inter laminar delamination cracks could be observed at the free edges but overall delamination remained negligible. Between 550 and 600 MPa, intralaminar cracks started to develop from the free edges in the 45° plies. Local delamination areas could be observed at that stage but were not able to propagate further. Finally, at 690 MPa, when nearly all intralaminar cohesive elements were fully damaged in the upper 45° ply, delamination cracks started to propagate from localized point on the free edge of the upper ply. Localized delamination cracks then developed on most interfaces in its surroundings. At 711 MPa, delamination cracks propagated suddenly and the fiber failure criterion of the 0° ply was reached close to the failure initiation point. Right after this local failure, an intralaminar crack propagated in the 0° ply and lead to extensive delamination. The type of final failure mode simulated by the model was found in good qualitative agreement with the experimental one (Fig. 4) in which final failure occurred by a combination of fiber fracture, 45° splits and 90° transverse cracking. Interestingly, comparison of the two models clearly shows that transverse cracking was significantly delayed in the intermediate ply specimen. Moreover, in the intermediate ply thickness laminate, no significant delamination could be observed before 98% of the ultimate stress while in the thick ply laminate delamination started at about 75% of ultimate strength.

The limited damage development in intermediate ply thickness laminate is also clearly visible on the total damage dissipation energy vs applied stress curves (Fig. 8). Interestingly these simulated curves compared reasonably well with the experimental cumulative acoustic energy vs stress curves. Using the simulated damage energy vs stress curves as indicators, the onset of damage of the thick and intermediate ply thickness specimens were estimated as 261 MPa and 457 MPa respectively. Indeed, this notable different shows that even though the same size independent constitutive properties were used in both cases, the models were able to capture at least part of the observed ply thickness effect just by representing the actual geometry, interfaces and 3D kinematics of the problem. Most importantly, to capture those thickness effects, it was verified that the model should be sufficiently refined to properly represent the geometry of the constrained transverse intra laminar cracks present in the +/-45° and 90° plies.

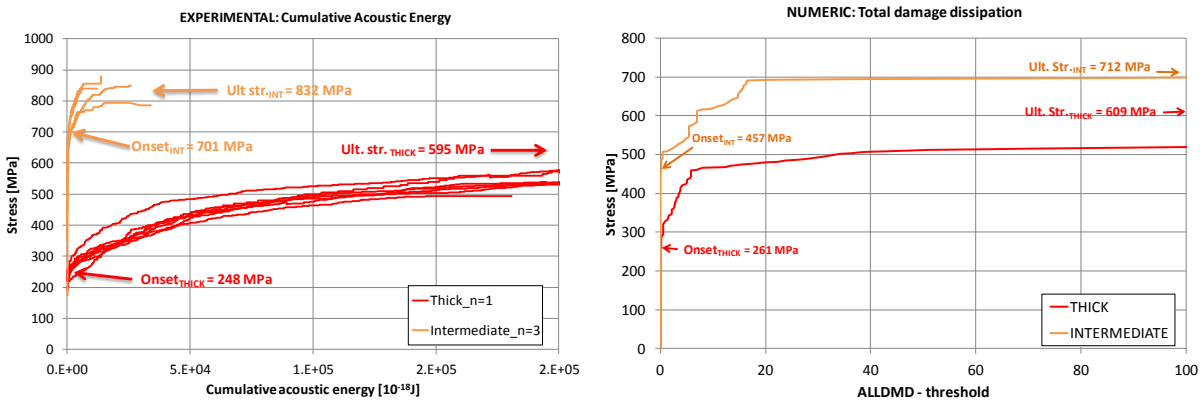


*Fig. 8: measured cumulative acoustic energy compared to simulated damage energy for thick and intermediate ply unnotched quasi-isotropic specimens.*

Comparing the numerical predictions to the experimentally determined onset of damage showed that the present model provided reliable values for the thick ply composite (261 MPa in FE, 248 MPa in experiment) but underestimated the ply-thickness effect significantly for the intermediate ply thickness (457 MPa in FE, 701 MPa in experiment). This difference could be partially attributable to the inherent difficulty of defining a meaningful threshold of damage or acoustic emission energy to determine the damage onset and to the selectivity of acoustic emission monitoring which could not record events with very low energy because of the noise rejection filter.

The ultimate strength predicted in the FE model of the thick-ply composite (609 MPa) matched well with the experiment (595 MPa). For intermediate ply thickness, the FE predictions of ultimate strength (712 MPa) were found to be in good qualitative agreement with experiments (832 MPa), showing the right trend towards an increase when decreasing ply thickness but failing to reproduce the measured values quantitatively (14% underestimation).

Additionally, the scaling in onset of damage with ply thickness $t$ obtained by the present FE model was compared to the theoretical scaling of linear elastic fracture mechanics (LEFM, scaling in $t^{-0.5}$) and experimental results (Fig 9). If the FE model predictions followed the theoretical LEFM scaling rather closely, both models were unable to represent the measured onset of damage of intermediate ply thickness. However, for thin plies, the LEFM theoretical scaling predicted a transverse cracking onset in good agreement with the experimental measurements, both very close to ultimate strength of the laminate.

According to the present experimental and numerical investigations, it is clear that the very significant change in onset of damage can be, at least partially, attributed to an increased stability of intra laminar transverse cracks in 90° and +/-45° plies near free edges while the ultimate strength seems to depend more on a complex interaction between delamination and transverse cracking. For thinner plies, damage propagation is overall hindered and very limited damage could develop until fiber failure happens in the 0° plies.

To illustrate this effect, classical laminate theory (CLT) was used to compute the first-ply failure and ultimate strength of the quasi isotropic specimens in unnotched tensile tests. Two extreme hypotheses were considered: (a) no damage of the ply was implemented in the CLT calculations and (b) plies become fully damaged (D=0.9999) as soon as it reaches the Tsai-Hill failure envelope. Ultimate strength was defined as the failure of the 0° ply. CLT calculations with damage provided an estimated first-ply failure at 287 MPa, in close agreement with the thick-ply onset of damage (248 MPa). The CLT model with damage of the plies led to ultimate strength prediction of 609 MPa close to the experimental values for the thick ply specimen (595 MPa). Interestingly, when no damage was considered, the ultimate strength obtained by CLT was 819 MPa and corresponded well with the values obtained in thin and intermediate ply thickness tests (832 MPa resp. 847 MPa). However, as shown before, damage progression was seriously limited for very thin ply composites and thus the traditionally

used first-ply failure criterion seemed irrelevant in those cases.

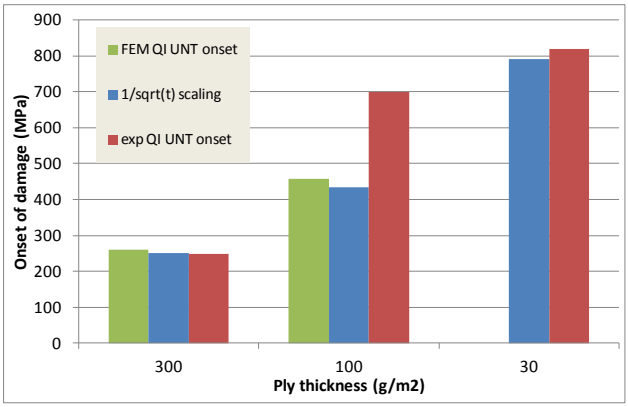


*Fig. 9: scaling of onset of damage stress vs ply thickness according to the present FE model, linear elastic fracture mechanics (scale as 1/sqrt(t)) and experiments*

This simple calculation example actually demonstrates, at least in the present case, that as most damage types are nearly suppressed when using very thin-ply composites, predicting their performance may actually be simpler than expected. Simple theories like CLT without ply and interfacial damage could thus be applicable when the ply thickness is "sufficiently" small (below a certain "critical ply thickness") as failure ends up being dominated by the ultimate strain in the fibers. However, further studies are required to verify if a "critical ply thickness" also exists for other types of laminates, fibers and matrix properties. Moreover, if it exists, a criterion to define the "critical ply thickness" in a given application would be highly valuable for design. To reach this stage of understanding, further studies would be required, for example, to improve and/or validate existing theories such as the in-situ strength model [5] or matrix cracking induced delamination criterion for a wider range of thin ply composites.

## 5. Conclusion

Ultra-thin ply composites are now becoming commercially available and are increasingly used in high end applications. As shown in this paper, reducing the ply thickness can lead to dramatic improvement in terms of first-ply / first-damage criteria but also in terms of fatigue life and ultimate strength. These significant improvements were related to a change in the failure mode: thin-ply composites exhibited a much delayed damage growth and showed a quasi-brittle failure instead of extensive delamination and transverse cracking patterns. Using 30g/m$^2$ plies in unnotched quasi isotropic tensile tests, it was shown that damage mechanisms could be delayed until the ultimate strain of the fiber was reached in the 0° ply.
Detailed meso-scale finite element models including transverse cracking, delamination and fiber failure damage mechanisms were able to represent the observed trends. The main cause of the strong enhancement in onset of damage when decreasing ply thickness appeared related to the increased stability of transverse intralaminar cracks caused by the constraining effects of the neighboring plies. The ultimate strength seemed related to a combination of factors including intra laminar cracking of the outer 45° plies and stability of the delamination cracks close to free edges. However, the number of sublaminate repetition was shown to play only a secondary role on the onset of damage and ultimate strength of unnotched thin-ply laminates. Even though existing theories based on fracture mechanics [5] and the present meso-scale FE models were both able to capture qualitatively the observed ply thickness effects, further developments are required to achieve more quantitative performance predictions and design rules of thin-ply composite parts.

## Acknowledgements

This work was sponsored by Swiss Commission for Technology and Innovation CTI project 127795.1 PFIW-IW in partnership with North-TPT, RUAG AG, Connova AG and IKT-FHNW.

## References

[1] S. Sihn, R.Y. Kim, K. Kawabe, S. Tsai, *"Experimental studies of thin-ply laminated composites"*, Composites Science and Technology, 67, 2007, pp. 996-1008
[2] M. R. Wisnom, "*Size effects in the testing of fibre-composite materials"*, Compos Sci and Technol, 59, 1999, pp 1937-1957
[3] M.R. Wisnom, B. Kahn, S.R. Hallet, *"Size effects in unnotched tensile strength of unidirectional and quasi-isotropic carbon/epoxy composites"*, Composite Structures, 84, 2008, pp. 21-28
[4] Sutherland, L.; Shenoi, R. & Lewis, S., *"Size and scale effects in composites: I. Literature review"*, Compos Sci and Technol, 59, 1999, pp. 209-220

[5] P. P. Camanho, C. G. Dávila, S. T. Pinho, L. Iannucci, P. Robinson, *"Prediction of in situ strengths and matrix cracking in composites under transverse tension and in-plane shear"*, Composites Part A, 37(2), 2006, pp.165-176
[6] E. Iarve, R. Kim, D. Mollenhauer, *"Three-dimensional stress analysis and Weibull statistics based strength prediction in open hole composites"*, Composites Part A, 38, 2007, pp. 174-185
[7] B.G. Green, M.R. Wisnom, S.R. Hallet, *"An experimental investigation into the tensile strength scaling of notched composites"*, Composites: Part A, 38, 2007, pp. 867-878
[8] M. R. Wisnom, S.Hallett, C. Soutis, *"Scaling effects in notched composites"*, J. Compos Materials, 44, 2010, pp. 195-210
[9] J. Lee, C. Soutis, *"A study on the compressive strength of thick carbon fibre-epoxy laminates"*, Compos Sci and Technol, 67, 2007, pp. 2015-2026
[10] J. Lee, C. Soutis, *"Measuring the notched compressive strength of composite laminates: Specimen size effects"*, Compos Sci and Technol, 68, 2008, pp. 2359-2366
[11] T. Yokozeki et al., *"Damage characterization in thin-ply composite laminates under out-of-plane transverse loadings"*, Composite Structures, 93, 2010, pp. 49–57
[12] T. Yokozeki et al., *"Experimental characterization of strength and damage resistance properties of thin-ply carbon fiber/toughened epoxy laminates"*, Composite Structures, 82, 2008, pp. 382–389
[13] J. B. Moon et al., *"Improvement of tensile properties of CFRP composites under LEO space environment by applying MWNTs and thin-ply"*, Composites: Part A, 42, 2011, pp. 694–701
[14] A. Arteiro, G. Catalanotti, J. Xavier, P.P. Camanho, *"Notched response of non-crimp fabric thin-ply laminates"*, Comp Sci Tech, 79, 2013, pp. 97-114